Investigation of Mode Coupling Due to Ohmic Wall Losses in Overmoded Uniform and Varying-Radius Circular Waveguides by the Method of Cross Sections

Jamal Shafii and Ronald J. Vernon, *Member, IEEE*

***Abstract*—The effect of ohmic wall losses on mode coupling in overmoded varying-radius circular waveguides is investigated. Mode coupling and multimode propagation in uniform lossy-wall circular waveguides is also discussed. The expressions for the coupling coefficients are given by line integrals of the power-normalized fields of the normal modes along the boundary of the waveguide cross section. Numerical results are presented for the case of propagation of an HE_{11}-like mode excitation in a uniform smooth lossy-wall circular waveguide.**

***Index Terms*—Hybrid HE_{11} mode, lossy-wall waveguides, method of cross sections, mode coupling, ohmic wall loss, overmoded waveguides.**

I. Introduction

HIGH-POWER transmission at millimeter-wave frequencies is normally accomplished in highly overmoded waveguides to reduce attenuation and avoid breakdown. This is especially important in many transmission and mode-conversion systems used with gyrotrons where high-order modes are often generated. In treating dissipated power in overmoded lossy-wall waveguides, one needs to take into account the interference of currents due to the different modes at the waveguide wall. In the past, inclusion of the effect of ohmic wall loss on propagating modes in overmoded waveguides was commonly treated by evaluating the attenuation constant of each mode individually by means of the power-loss method, and the coupling mechanism was assumed to be nondissipative [1]. It is sometimes incorrect to treat the attenuation of individual modes separately in a multimode waveguide because the relative phase of the modes present can have a strong effect on the power dissipated. The conventional power-loss approach in evaluating the attenuation constants of modes individually will give smoothly decaying power loss along the waveguide, which is not always correct. In this paper, we extend and verify a formulation of the coupled-mode formalism [2], [3], which correctly predicts the power dissipated in the waveguide wall. We derive the effect of ohmic wall losses on the coupling coefficients in a varying-radius circular waveguide and discuss mode coupling and multimode propagation in a uniform lossy-wall waveguide.

We represent the fields at any cross section of a lossy-wall varying-radius guide as a superposition of the fields of the modes of a uniform guide of the same cross section, but with a perfectly conducting wall. The mode amplitudes along the guide are shown to be described by a system of first-order coupled ordinary differential equations. The coefficients of this system are called the coupling coefficients. This method of derivation of the coupling coefficients is sometimes called the method of cross sections. This method has been used in analyzing mode coupling in waveguides with different types of wall nonuniformities such as waveguides with a varying-radius wall profile for the case of azimuthally symmetric transverse electric modes [2], [4], corrugated and smooth-wall waveguides with various wall distortion [5], [6], and coaxial waveguides with varying radius center and outer conductors [7].

The integral expressions for the coupling coefficients are derived in Section II. In Section III, the solution of the coupled-mode equations for uniform lossy-wall waveguides is discussed. The dissipated power at the wall predicted by the coupled-mode equations and the power-loss formula is compared in Section IV. Some numerical results for multimode propagation and power loss for an HE_{11}-like combination of modes are given in Section V, followed by concluding remarks in Section VI.

II. Integral Expressions for the Coupling Coefficients in Varying-Radius Circular Waveguides With Ohmic Wall Losses

We assume that the axis of the varying-radius waveguide coincides with the z axis of the cylindrical coordinate system ρ, ϕ, and z and that the guide is homogeneously filled with an isotropic lossless medium, the plane wavenumber of which is $k = \omega\sqrt{(\mu\epsilon)}$, where μ and ϵ are the permeability and the permittivity, respectively, of the medium inside the guide. The wall of the guide is a slightly lossy conductor. The time variation is taken to be $e^{j\omega t}$.

The boundary conditions at the wall of the guide are

$$E_\phi = Z_w \cos\theta (H_z + H_\rho \tan\theta) \tag{1a}$$

$$E_z + E_\rho \tan\theta = -\frac{Z_w}{\cos\theta} H_\phi \tag{1b}$$

Manuscript received February 17, 2001. This work was supported by the U.S. Department of Energy under Grant DE-FG02-85ER52122.

The authors are with the Department of Electrical and Computer Engineering, University of Wisconsin–Madison, Madison, WI 53706 USA.

Publisher Item Identifier S 0018-9480(02)04058-9.

where Z_w is the surface impedance of the conducting wall, and θ is the angle that a line tangent to the wall makes with the z axis. The approximate boundary conditions above are valid if $Z_w \ll \eta$, where $\eta = \sqrt{(\mu/\epsilon)}$ is the intrinsic impedance of the medium filling the guide, and $Z_w \ll \eta k a_c$, where a_c is the smallest radius of curvature of the wall [8]. Furthermore, the skin depth of the conducting wall must be much smaller than the wall thickness.

We consider some cross section of the varying-radius waveguide $S = S_o$ at $z = z_o$ and construct a uniform waveguide with a perfectly conducting wall with the same local cross section S_o. We then expand the fields of the varying-radius guide at $z = z_o$ in terms of the normalized fields of the modes of the uniform guide as follows:

$$\begin{aligned} \mathbf{E}_t &= \sum_\tau V_\tau(z)\tilde{\mathbf{e}}_{t\tau}(\rho,\,\phi) \\ E_z &= \sum_\tau v_\tau(z)\tilde{e}_{z\tau}(\rho,\,\phi) \end{aligned} \tag{2}$$

$$\begin{aligned} \mathbf{H}_t &= \sum_\tau I_\tau(z)\tilde{\mathbf{h}}_{t\tau}(\rho,\,\phi) \\ H_z &= \sum_\tau i_\tau(z)\tilde{h}_{z\tau}(\rho,\,\phi). \end{aligned} \tag{3}$$

Here, $\tilde{\mathbf{e}}_\tau(\rho,\,\phi)$ and $\tilde{\mathbf{h}}_\tau(\rho,\,\phi)$ are only functions of the transverse coordinates. The positive integers τ and ν are used as indexes for the eigenmodes. Furthermore, the subscripts t and z, respectively, denote the transverse and z-directed components of the fields. The "$\sim$" over the functions in (2) and (3) indicates that these functions are normalized such that they satisfy the following orthogonality relations:

$$\begin{aligned} \iint_{S_o} \tilde{\mathbf{e}}_{t\tau}\cdot\tilde{\mathbf{e}}^*_{t\nu}\,dS &= \delta_{\tau\nu} \\ \iint_{S_o} \tilde{e}_{z\tau}\tilde{e}^*_{z\nu}\,dS &= \delta_{\tau\nu} \end{aligned} \tag{4}$$

$$\begin{aligned} \iint_{S_o} \tilde{\mathbf{h}}_{t\tau}\cdot\tilde{\mathbf{h}}^*_{t\nu}\,dS &= \delta_{\tau\nu} \\ \iint_{S_o} \tilde{h}_{z\tau}\tilde{h}^*_{z\nu}\,dS &= \delta_{\tau\nu} \end{aligned} \tag{5}$$

where the superscript $*$ denotes the complex conjugate. Due to the normalization relations (4) and (5), the complex power flow in each mode τ is $P_\tau = V_\tau I^*_\tau$. The series expansions (2) and (3) do not converge uniformly. For example, $\tilde{e}_{\phi\tau}$ and $\tilde{e}_{z\tau}$ vanish at the wall of the guide, but according to (1a) and (1b), E_ϕ and E_z do not. Therefore, we have been cautious not to take term-by-term differentiation of the infinite series (2) and (3) in the derivation of the coupled-mode equations. (Otherwise, the derivation of the coupling coefficients would have been valid only when the series expansions (2) and (3) converge uniformly. This would have put the following constraint on the nonuniform waveguide as seen form the boundary conditions of (1): 1) the guide wall of the nonuniform waveguide must be everywhere almost parallel to the guide axis (i.e., the rate of change of the guide cross section $(\tan\theta)$ must be very small) and 2) Z_w must be very small.)

The system of coupled differential equations that describe the complex coefficients V_τ and I_τ of series expansions (2) and (3) can be obtained from Maxwell's curl equations and the boundary conditions (1)

$$\frac{dV_\nu}{dz} = -jZ_\nu\beta_\nu I_\nu + \sum_\tau C_{\nu\tau}V_\tau + \sum_\tau R^v_{\nu\tau}I_\tau \tag{6a}$$

$$\frac{dI_\nu}{dz} = -j\,\frac{\beta_\nu}{Z_\nu}\,V_\nu - \sum_\tau C^*_{\tau\nu}I_\tau + \sum_\tau R^i_{\nu\tau}V_\tau \tag{6b}$$

where

$$C_{\nu\tau} = \iint_{S_o} \tilde{\mathbf{e}}_{t\tau}\cdot\frac{\partial}{\partial z}\,\tilde{\mathbf{e}}^*_{t\nu}\,dS \tag{7}$$

$$R^v_{\nu\tau} = -\frac{Z_w}{\cos\theta}\oint \tilde{h}^*_{\phi\nu}\tilde{h}_{\phi\tau}\,dl \tag{8a}$$

$$R^i_{\nu\tau} = \frac{k_\nu k_\tau}{(j\omega\mu)^2}\,Z_w\cos\theta\oint \tilde{h}^*_{z\nu}\tilde{h}_{z\tau}\,dl. \tag{8b}$$

Here, β_ν, Z_ν, and k_ν are the phase constant, the transverse wave impedance, and the cutoff wavenumber, respectively, of mode ν in the lossless uniform waveguide with cross section S_o. In (7), the integral is taken over the cross section of the guide and, in (8), the line integral is along the perimeter of the unperturbed waveguide cross section. Furthermore, in (8), $dl = a\,d\phi$, where a is the waveguide radius at the local cross section S_o.

For our purposes, it is convenient to write the coupled-mode equations not in terms of the modal voltage and current, but in terms of the normalized complex amplitudes of the forward and backward propagating modes. The relation between these two formalism is as follows:

$$\begin{aligned} V_\nu &= \sqrt{Z_\nu}\left(A^+_\nu + A^-_\nu\right) \\ I_\nu &= \frac{1}{\sqrt{Z_\nu}}\left(A^+_\nu - A^-_\nu\right). \end{aligned} \tag{9}$$

The power transported in the $+\hat{\mathbf{a}}_z$-direction by the νth mode is given by $|A^+_\nu|^2$ and that in the $-\hat{\mathbf{a}}_z$-direction by $|A^-_\nu|^2$.

If V_ν and I_ν in (6) are represented in terms of A^+_ν and A^-_ν, we may obtain the coupled-mode equations for the forward and backward propagating modes in a varying-radius guide with ohmic wall loss

$$\frac{dA^+_\nu}{dz} = -j\beta_\nu A^+_\nu + \sum_\tau\left(\kappa^+_{\nu\tau} + S^+_{\nu\tau}\right)A^+_\tau + \sum_\tau\left(\kappa^-_{\nu\tau} + S^-_{\nu\tau}\right)A^-_\tau \tag{10a}$$

$$\frac{dA^-_\nu}{dz} = +j\beta_\nu A^-_\nu + \sum_\tau\left(\kappa^-_{\nu\tau} - S^-_{\nu\tau}\right)A^+_\tau + \sum_\tau\left(\kappa^+_{\nu\tau} - S^+_{\nu\tau}\right)A^-_\tau. \tag{10b}$$

Here, the coupling coefficients $S^\pm_{\nu\tau}$ are given by

$$S^\pm_{\nu\tau} = -\frac{1}{2}\cos\theta\oint Z_w h^*_{z\nu}h_{z\tau}\,dl \mp \frac{1}{2}\,\frac{1}{\cos\theta}\oint Z_w h^*_{\phi\nu}h_{\phi\tau}\,dl \tag{11}$$

and the coupling coefficients $\kappa^\pm_{\nu\tau}$ are given below.

If both ν and τ represent TE modes or TM modes

$$\kappa_{\nu\tau}^{\pm} = \frac{1}{2}\frac{1}{\beta_\nu \mp \beta_\tau}\oint \tan\theta \cdot \left(\omega\mu h_{z\nu}^* h_{z\tau} \pm \omega\mu h_{\phi\nu}^* h_{\phi\tau} - \omega\epsilon e_{\rho\nu}^* e_{\rho\tau}\right) dl, \qquad \nu \neq \tau \tag{12a}$$

$$\kappa_{\tau\tau}^{-} = -\frac{1}{2}\oint \tan\theta h_{\phi\tau}^* e_{\rho\tau}\, dl - \frac{1}{2}\frac{1}{Z_\tau}\frac{dZ_\tau}{dz}$$
$$\kappa_{\tau\tau}^{+} = 0. \tag{12b}$$

If ν is a TE mode and τ is a TM mode

$$-\kappa_{\nu\tau}^{+} = \kappa_{\nu\tau}^{-} = \kappa_{\tau\nu}^{\pm *} = -\frac{1}{2}\oint \tan\theta e_{\rho\nu}^* h_{\phi\tau}\, dl. \tag{13}$$

In the above equations, $\mathbf{e}_\tau(\rho, \phi)$ and $\mathbf{h}_\tau(\rho, \phi)$ are, respectively, the power-normalized electric and magnetic fields given by

$$\mathbf{e}_{t\tau} = \sqrt{Z_\tau}\tilde{\mathbf{e}}_{t\tau}$$
$$e_{z\tau} = \frac{1}{j\omega\epsilon}\frac{1}{\sqrt{Z_\tau}} k_\tau \tilde{e}_{z\tau} \tag{14}$$

$$\mathbf{h}_{t\tau} = \frac{1}{\sqrt{Z_\tau}}\tilde{\mathbf{h}}_{t\tau}$$
$$h_{z\tau} = \frac{1}{j\omega\mu}\sqrt{Z_\tau} k_\tau \tilde{h}_{z\tau}. \tag{15}$$

The fields above satisfy the power normalization

$$\left|\iint_{S_o} (\mathbf{e}_{t\tau} \times \mathbf{h}_{t\tau}^*)\cdot \hat{\mathbf{a}}_z\, dS\right| = 1. \tag{16}$$

In the derivation of the coupling coefficients, the higher order terms in Z_w have been neglected since their effect is negligible for good conductors.

The coupled-mode equations (10) are valid in a varying-radius waveguide with a slowly varying cross section [7]. In the voltage–current formulation (6), it is not necessary to require the slowly varying constraint if a sufficient number of evanescent modes are included [9].

We notice that the $S_{\nu\tau}^{\pm}$ arise from the wall loss and the $\kappa_{\nu\tau}^{\pm}$ arise due to the radius variation. We also notice from (11) that the coupling due to ohmic loss is dependent on θ, the angle that the waveguide wall makes with the z axis. The coupling coefficients $\kappa_{\nu\tau}^{\pm}$ are the same as the coupling coefficients for the case of a perfectly conducting varying-radius circular waveguide [5], [10].

In this paper, we have only considered a varying-radius perturbation. For more general deformations with the guide wall described by $a(z) + \delta(\phi, z)$, where $\delta \ll a$, such as waveguides with ellipticity, curvature, or multifoil perturbations, the boundary conditions in (1) and the coupling coefficients due to loss in (8) or (11) are still valid to the zeroth order in δ. The next higher order term is one order of magnitude smaller in δ. Thus, for coupling due to losses, the wall perturbations arising from δ can be neglected for small δ even though δ may produce significant "lossless" coupling.

In a circular waveguide, the single-mode numbers ν or τ take the place of the entire TE_{mn}- or TM_{mn}-mode designation. The expressions for the mode functions $\tilde{\mathbf{e}}_\tau(\rho, \phi)$ and $\tilde{\mathbf{h}}_\tau(\rho, \phi)$ of TE and TM modes in a lossless uniform circular waveguide can be found in [11]. In our calculations and analysis in this paper, the expressions for the field components are chosen such that the sign of the radial function part of $\tilde{h}_{\phi,mn}$ is positive at the wall for both TE_{mn} and TM_{mn} modes.

From the integral equations (11)–(13), for coupling due to wall loss and/or radius variation, we can make the following general statements.

1) Only modes with the same azimuthal index m couple to each other.
2) For stationary modes, only modes with the same "polarization," i.e., either $h_{\phi,mn} \propto \sin(m\phi)$ or $h_{\phi,mn} \propto \cos(m\phi)$ couple to each other.
3) For rotating modes, only modes with the same sense of rotation, i.e., either $h_{\phi,mn} \propto \exp(jm\phi)$ or $h_{\phi,mn} \propto \exp(-jm\phi)$ couple to each other.
4) TE_{0n} and TM_{0n} modes are not coupled to each other.

III. Solution of the Coupled-Mode Equations in a Uniform Lossy-Wall Waveguide

In the remainder of this paper, we will focus only on uniform waveguides ($\theta = 0$) made of conducting walls that are slightly lossy with Z_w being the surface impedance of the wall. Here, the coupling mechanism arises only due to the resistive nature of the waveguide wall and, hence, the coupling coefficients are constant along the uniform waveguide. We will also neglect the backward propagating modes. We will show in Section V that neglecting the backward coupled modes is a justifiable approximation, except when incident modes are propagating very close to cutoff.

We will solve the coupled-mode equations in the following form:

$$\overline{\boldsymbol{A}}(z) = [\boldsymbol{M}(z)]\overline{\boldsymbol{A}}_o \tag{17}$$

where the transmission matrix $[\boldsymbol{M}(z)]$ gives the value of the complex amplitude vector $\overline{\boldsymbol{A}}(z)$ at any point z in terms of the known initial amplitudes $\overline{\boldsymbol{A}}_o$ at $z = 0$. The column vector $\overline{\boldsymbol{A}}$ consists of the complex mode amplitudes A_ν, where $\nu = 1, 2, 3, \ldots$, as its components.

Below, we present the analysis for only two modes, although the procedure and the concepts can be applied to any number of modes. The coupled-mode equations for two forward propagating modes in a uniform waveguide with ohmic wall loss are obtained from (10) and (11) and are as follows:

$$\frac{d}{dz}\overline{\boldsymbol{A}} = [\boldsymbol{G}]\overline{\boldsymbol{A}} \tag{18}$$

and are as shown in (19a)–(19c) at the bottom of the following page, where R_w is the real part of Z_w. In (19b), $h_{z\nu}$ and $h_{\phi\nu}$, $\nu = 1, 2$ are the axial and azimuthal components, respectively, of the power normalized magnetic fields of the νth mode at the wall. We notice that the "attenuation constant" and "phase constant" matrices are Hermitian, i.e.,

$$[\alpha] = [\alpha]^\dagger \text{ and } [\beta] = [\beta]^\dagger \tag{20}$$

where † denotes the transpose and conjugation.

To solve the coupled-mode equations (18) for the unknown $\overline{\boldsymbol{A}}(z)$ with a given initial condition $\overline{\boldsymbol{A}}_o$ at $z=0$, we suppose that the 2×2 matrix $[\boldsymbol{G}]$ has two linearly independent eigenvectors and these vectors are chosen to be the columns of a 2×2 matrix $[\boldsymbol{Q}]$. Then, by using the change of variables

$$\overline{\boldsymbol{A}} = [\boldsymbol{Q}]\bar{\mathbf{a}}. \tag{21}$$

Equation (18) reduces to

$$\frac{d}{dz}\bar{\mathbf{a}} = -[\Lambda]\bar{\mathbf{a}} \tag{22a}$$

where

$$[\Lambda] = [\boldsymbol{Q}]^{-1}[\boldsymbol{G}][\boldsymbol{Q}] = \begin{bmatrix} \gamma_1 & 0 \\ 0 & \gamma_2 \end{bmatrix} \tag{22b}$$

is a diagonal matrix with the eigenvalues of $[\boldsymbol{G}]$ along its diagonal. The eigenvalues can be obtained as follows:

$$\gamma_1 = \mu_1 + \mu_2 \text{ and } \gamma_2 = \mu_1 - \mu_2 \tag{23a}$$

where

$$\mu_1 = \frac{1}{2}(G_{11}+G_{22}) \tag{23b}$$

$$\mu_2 = \frac{1}{2}\sqrt{(G_{11}-G_{22})^2 + 4G_{12}G_{21}}. \tag{23c}$$

The eigenvalues γ_1 and γ_2 above are distinct; hence, the two corresponding eigenvectors are automatically independent [12]. Therefore, the diagonalization above is possible.

The change of variables by (21) implies that the eigenvectors of $[\boldsymbol{G}]$ are chosen as the new basis vectors. The column vector $\bar{\mathbf{a}}$ consists of the complex amplitudes $\mathbf{a}_\nu$, where $\nu = 1, 2$ of the new set of modes as its components. The new set of modes are actually the eigenmodes of the lossy-wall waveguide.

The system (22a) is uncoupled and the new normal modes with complex amplitudes $\mathbf{a}_1$ and $\mathbf{a}_2$ propagate independently. However, the coupling matrix $[\boldsymbol{G}]$ is not normal, i.e., it does not commute with its conjugate transpose. Therefore, its eigenvectors are not orthogonal [12]. Hence, although the new basis vectors are independent, they are not orthogonal. This shows that, although the new modes with complex amplitudes $\mathbf{a}_1$ and $\mathbf{a}_2$ are uncoupled, they are not power orthogonal, i.e., the total power transported by the new modes is not the sum of the powers carried by each mode individually. In confirmation of this statement, we have shown independently in another place that the eigenmodes of lossy-wall uniform waveguides are not power orthogonal [13]. When the modes are degenerate, i.e., when in (19c) $\beta_1 = \beta_2$, $[\boldsymbol{G}]$ is normal. Thus, for degenerate modes only, the new modes are not only decoupled, but they are also power orthogonal. This conclusion is consistent with the previous work done by Gustincic [14] and Collin [15] where they show that when a set of modes are degenerate in a uniform lossy-wall waveguide, a new set of modes can be obtained by linear combination of the original degenerate modes such that these new modes are uncoupled, as well as power orthogonal. It should be emphasized that the coupled-mode formulation developed above is valid for both degenerate and nondegenerate modes.

By combining (21) and (22), the transmission matrix $[\boldsymbol{M}(z)]$ is

$$[\boldsymbol{M}] = [\boldsymbol{Q}]e^{-[\Lambda]z}[\boldsymbol{Q}]^{-1} \tag{24a}$$

where

$$e^{-[\Lambda]z} = \begin{bmatrix} e^{-\gamma_1 z} & 0 \\ 0 & e^{-\gamma_2 z} \end{bmatrix}. \tag{24b}$$

The explicit expressions for the elements of the transmission matrix are

$$M_{11} = \frac{1}{2\mu_2}e^{-\mu_1 z}\left[2\mu_2\cosh(\mu_2 z) - (G_{11}-G_{22})\sinh(\mu_2 z)\right] \tag{25a}$$

$$M_{12} = -\frac{1}{\mu_2}G_{12}e^{-\mu_1 z}\sinh(\mu_2 z) \tag{25b}$$

$$M_{21} = -\frac{1}{\mu_2}G_{21}e^{-\mu_1 z}\sinh(\mu_2 z) \tag{25c}$$

$$M_{22} = \frac{1}{2\mu_2}e^{-\mu_1 z}\left[2\mu_2\cosh(\mu_2 z) + (G_{11}-G_{22})\sinh(\mu_2 z)\right]. \tag{25d}$$

IV. Comparison of Dissipated Power Obtained by the Coupled-Mode Equations and the Power-Loss Method

In this section, we use (17) to calculate the ohmic power loss per unit length. We then show that when more than one mode

$$\lfloor \boldsymbol{G} \rfloor = \lfloor \alpha \rfloor + j\lfloor \beta \rfloor \tag{19a}$$

$$[\alpha] = \begin{bmatrix} \frac{1}{2}\oint R_w\left(|h_{z1}|^2+|h_{\phi 1}|^2\right)dl & \frac{1}{2}\oint R_w\left(h_{z1}^* h_{z2} + h_{\phi 1}^* h_{\phi 2}\right)dl \\ \frac{1}{2}\oint R_w\left(h_{z1}h_{z2}^* + h_{\phi 1}h_{\phi 2}^*\right)dl & \frac{1}{2}\oint R_w\left(|h_{z2}|^2+|h_{\phi 2}|^2\right)dl \end{bmatrix} \tag{19b}$$

$$[\beta] = \begin{bmatrix} \beta_1 & 0 \\ 0 & \beta_2 \end{bmatrix} + [\alpha] \tag{19c}$$

propagates in the waveguide, the coupled-mode equations predict that the power loss per unit length varies along the waveguide due to the interference of the modal currents in the wall. We will also derive the dissipated power by the power-loss formula and show that the two methods above give the same result over a very short waveguide length. This agreement is a partial validation of the coupled-mode equation method.

The total power carried by modes at any cross section is $P = \overline{\boldsymbol{A}}^{\dagger}\overline{\boldsymbol{A}}$. The power loss per unit length can then be determined by making use of the coupled-mode equations (18) and relations (20) to obtain

$$-\frac{dP}{dz} = 2\overline{\boldsymbol{A}}^{\dagger}[\alpha]\overline{\boldsymbol{A}} \tag{26}$$

which can be expressed in terms of the input vector $\overline{\boldsymbol{A}}_o$ as follows:

$$-\frac{dP}{dz} = 2\overline{\boldsymbol{A}}_{\boldsymbol{o}}^{\dagger}\Big([\boldsymbol{M}]^{\dagger}[\alpha][\boldsymbol{M}]\Big)\overline{\boldsymbol{A}}_o. \tag{27}$$

Notice that only $[\alpha]$ appears in the above equation for the power loss. This is because the $j[\beta]$ part of coupling matrix $[\mathbf{G}]$ is anti-Hermitian and, hence, it does not contribute to loss. For the two-mode problem, (26) yields, in terms of the elements of $[\alpha]$

$$-\frac{dP}{dz} = 2\Big(\alpha_{11}|A_1|^2 + \alpha_{22}|A_2|^2 + \alpha_{12}A_1^*A_2 + \alpha_{12}^*A_1A_2^*\Big). \tag{28}$$

Each of the first two terms on the right-hand side of the relation above arises only due to the magnitude of a single modal amplitude. The last two terms, however, arise from the coupling effect due to the wall loss, and their values depend on the magnitudes of both modes, as well as their relative phases. Hence, at locations along the waveguide where the modes are out-of-phase (by our convention), power loss is small, but where the modes are in-phase, power loss is larger. Thus, depending on the relative phases of the modes, ohmic loss may be minimal at some locations, while at others, the dissipated power may be appreciable.

The power loss can also be calculated by the following formula:

$$\int_0^z \int_0^{2\pi} R_w|\mathbf{J_s}|^2 a\, d\phi\, dz \tag{29}$$

where $\mathbf{J_s}$ is the rms surface current that is obtained from the total tangential magnetic field at the wall, and a is the waveguide radius. We will show that (28) and (29) yield the same result for the dissipated ohmic power at the wall over a short length δz. Assume that the two modes have the following magnetic field components tangent to the wall:

$$H_{\phi\nu} = A_{\nu o}h_{\phi\nu}e^{-j\beta_\nu z} \text{ and } H_{z\nu} = A_{\nu o}h_{z\nu}e^{-j\beta_\nu z} \tag{30}$$

where $\nu = 1, 2$. The fields above are normalized such that the power carried by the νth mode is $|A_{\nu o}|^2$. The surface current at the wall is $\mathbf{J_s} = \mathbf{H} \times \hat{\mathbf{a}}_\rho$, where $\mathbf{H}$ is now the total magnetic field. The power loss over a short distance δz can be derived explicitly from (29) and (30) as follows:

$$\begin{aligned}
&\int_0^{\delta z}\int_0^{2\pi} R_w|\mathbf{J_s}|^2 a\, d\phi\, dz \\
&= aR_w\int_0^{2\pi}\Bigg\{\Big[|A_{1o}|^2\left(|h_{\phi 1}|^2+h_{z1}|^2\right) \\
&\qquad +|A_{2o}|^2\Big(|h_{\phi 2}|^2+|h_{z2}|^2\Big)\Big]\,\delta z \\
&\qquad +\frac{\sin\left(\dfrac{\beta_1-\beta_2}{2}\,\delta z\right)}{\dfrac{\beta_1-\beta_2}{2}} \\
&\qquad \cdot\Big[e^{-j((\beta_1-\beta_2)/2)\delta z}A_{1o}A_{2o}^*\big(h_{\phi 1}h_{\phi 2}^*+h_{z1}h_{z2}^*\big) \\
&\qquad\quad +e^{j((\beta_1-\beta_2)/2)\delta z}A_{1o}^*A_{2o}(h_{\phi 1}^*h_{\phi 2} \\
&\qquad\qquad +h_{z1}^*h_{z2})\Big]\Bigg\}\,d\phi.
\end{aligned} \tag{31}$$

Over a very short waveguide length δz, the modal magnetic fields of a lossless waveguide (30) may be used here since the modal fields are not significantly perturbed by the wall loss. Thus, the dissipated power can be obtained from (31) by letting δz approach zero as follows:

$$\begin{aligned}
&\lim_{\delta z\to 0}\int_0^{\delta z}\int_0^{2\pi} R_w|\mathbf{J_s}|^2 a\, d\phi\, dz \\
&= 2\Big[\Big(\alpha_{11}|A_{1o}|^2+\alpha_{22}|A_{2o}|^2\Big) \\
&\qquad +\Big(\alpha_{12}^*A_{1o}A_{2o}^*+\alpha_{12}A_{1o}^*A_{2o}\Big)\Big]\,\delta z.
\end{aligned} \tag{32}$$

Notice that (28) and (32) yield the same result for the dissipated power.

V. Numerical Results for Propagation of an HE_{11}-Like Mode

The hybrid HE_{11} mode in a corrugated circular waveguide is an ideal mode for waveguide transmission systems [16], [17]. It is suited for low-loss transmission due to its very low attenuation. It also has a Gaussian-like radiation pattern when it is radiated from an open-ended waveguide and, hence, it couples strongly to the fundamental Gaussian free-space mode. The HE_{11} mode can be expanded in terms of the TE_{1n} and TM_{1n} modes of a smooth-wall waveguide at any given transverse plane. However, it can reasonably be represented by only the TE_{11} and TM_{11} modes with power compositions of approximately 85% and 15%, respectively, and a phase difference of 180° at the waveguide wall. When the two modes are out-of-phase, the azimuthal components of the magnetic fields of the two modes almost cancel each other at the waveguide wall, which leads to the overall low ohmic loss.

For our study, we assume that the mode mixture above is injected into a uniform smooth lossy-wall circular waveguide. In Table I, we compare the results of the dissipated power over

TABLE I
DISSIPATED POWER IN A LOSSY-WALL CIRCULAR WAVEGUIDE (OVER A LENGTH d) FOR A TE_{11} AND- TM_{11}-MODE MIXTURE (POWER COMPOSITION: 85% TE_{11} AND 15% TM_{11}, WAVEGUIDE DIAMETER $= 0.64$ cm, FREQUENCY $= 60$ GHz, WALL CONDUCTIVITY $= 7 \times 10^4$ S/m)

	Modes in phase		Modes out of phase	
length (d)	Coupled mode equations	Power-loss formula	Coupled mode equations	Power-loss formula
$\lambda/5$	5.4957×10^{-3}	5.5218×10^{-3}	1.1324×10^{-3}	1.1340×10^{-3}
$\lambda/10$	2.8320×10^{-3}	2.8391×10^{-3}	4.8863×10^{-4}	4.8885×10^{-4}
$\lambda/50$	5.7266×10^{-4}	5.7295×10^{-4}	9.2626×10^{-5}	9.2632×10^{-5}

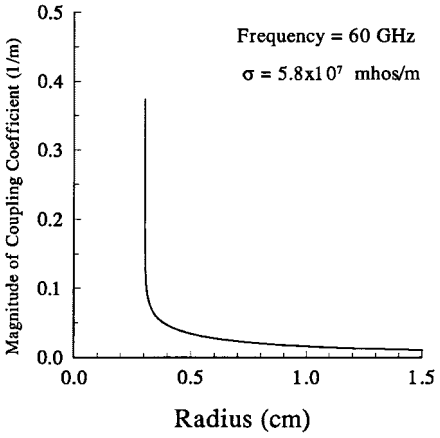

Fig. 1. Magnitude of the TE_{11}–TM_{11} coupling coefficient due to ohmic wall loss versus the guide radius in a circular waveguide assuming a surface resistivity of ideal copper. The cutoff radius for the TM_{11} mode is 0.3047 cm.

different waveguide lengths calculated from the coupled-mode formulation and the power-loss formula (31) for a waveguide with the wall resistivity of graphite. We notice that the calculated values from the two methods converge as the waveguide length becomes much smaller than the free-space wavelength. In this table, we have also listed the results for the case where, at the input of the waveguide section, the azimuthal components of the magnetic fields of the two modes are in-phase and, hence, they add at the wall. The power dissipated in a small length is almost five times greater for this case.

The injected TE_{11} and TM_{11} modes considered above couple energy due to the lossy nature of the wall. The coupling coefficient $-G_{12}$ can be calculated from (19), and its magnitude has been plotted versus the waveguide radius in Fig. 1 for a circular copper waveguide with an input signal of 60 GHz. As observed in this figure, near the cutoff radius of the TM_{11} mode, the coupling coefficient becomes very large. In a uniform waveguide with its radius in this region, the backward coupled TE_{11} and TM_{11} modes will be excited with appreciable amplitude. Furthermore, higher order TE_{1n} and TM_{1n} evanescent modes may also be excited with small amplitude. However, coupling to these modes is not included in the coupled-mode formulation (18).

As was mentioned in Section III, the modes described by $\bar{\mathbf{a}}$ in (22) define the eigenmodes of a uniform lossy-wall waveguide

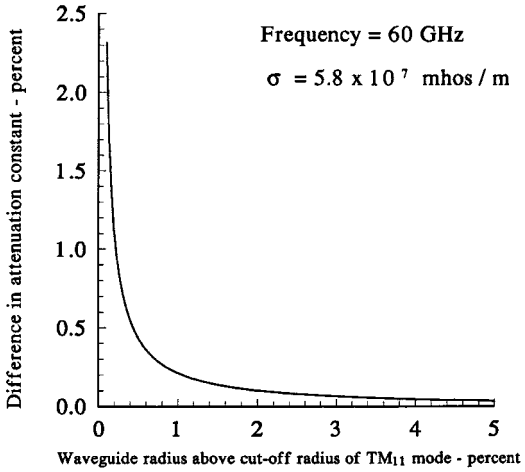

Fig. 2. Percent difference between the TM_{11} attenuation constant calculated by the coupled-mode equations and by the eigenmode expansion method assuming a surface resistivity of ideal copper. Ten TE_{1n} and ten TM_{1n} modes are included for the eigenmode expansion method.

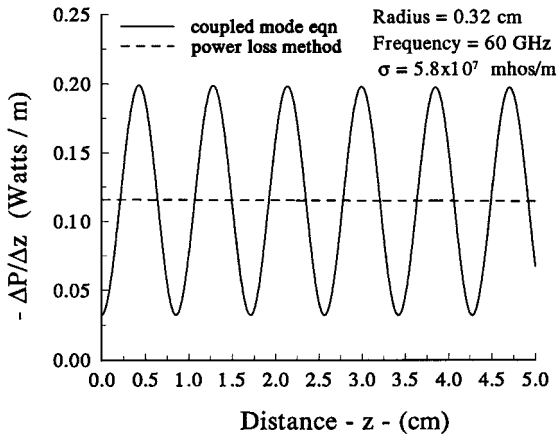

Fig. 3. Power loss per unit length along a lossy-wall circular waveguide with a 0.64-cm diameter assuming a surface resistivity of ideal copper. The TE_{11} and TM_{11} modes are injected at $z = 0$ with a power composition of 85% and 15%, respectively, and a phase difference of 180°.

with γ_1 and γ_2 as their propagation constants. Therefore, we can check the validity of the coupled-mode equations (18) near the cutoff radius of the TM_{11} mode by comparing γ_2 with that obtained by other methods for obtaining the propagation constants of eigenmodes of uniform smooth lossy-wall waveguides such as the eigenmode expansion method [18] or Jackson's perturbational analysis method [19]. In Fig. 2, we have plotted the percent difference between the attenuation constant of the TM_{11} mode calculated by (23) and by the eigenmode expansion method where ten TE_{1n} and ten TM_{1n} modes were used. This figure shows that there is only 2% deviation in the attenuation constant when the waveguide radius is only 0.1% above cutoff. Hence, we believe that the coupled-mode equations (18) correctly represent the interaction of modes due to wall loss when the waveguide radius is larger than 0.1% above the cutoff radius of the TM_{11} mode. If the backward, as well as the forward propagating TE_{11} and TM_{11} modes are used in the coupled-mode equations, this restriction can be relaxed, i.e., in this case, the waveguide radius may be chosen to be closer to the TM_{11} cutoff

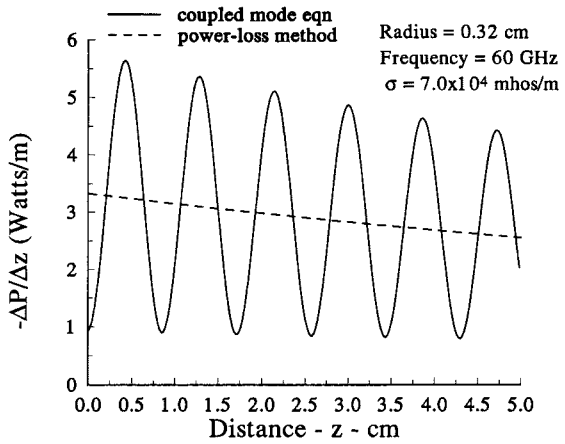

Fig. 4. Power loss per unit length along a lossy-wall circular waveguide with a 0.64-cm diameter assuming a surface resistivity of ideal graphite. The TE_{11} and TM_{11} modes are injected at $z = 0$ with a power composition of 85% and 15%, respectively, and a phase difference of 180°.

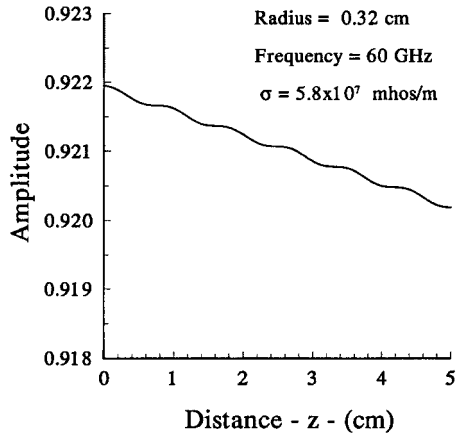

Fig. 5. Amplitude of the TE_{11} mode (of the TE_{11} and TM_{11} combination) along the lossy-wall circular waveguide with 0.64-cm diameter assuming a surface resistivity of ideal copper.

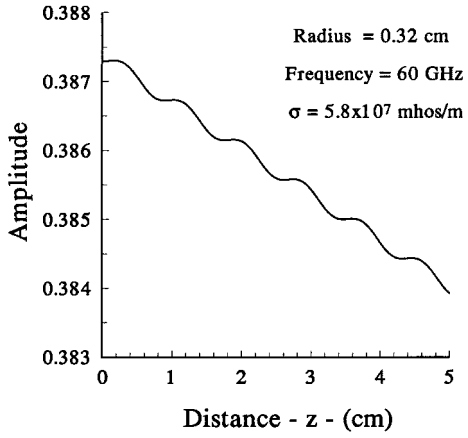

Fig. 6. Amplitude of the TM_{11} mode (of the TE_{11} and TM_{11} combination) along the lossy-wall circular waveguide with 0.64-cm diameter assuming a surface resistivity of ideal copper.

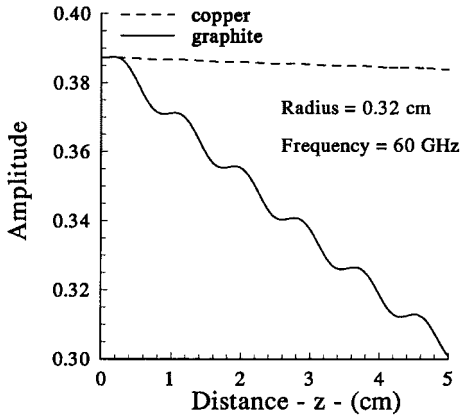

Fig. 7. Amplitude of the TE_{11} mode (of the TE_{11} and TM_{11} combination) along the lossy-wall circular waveguide with 0.64-cm diameter for both copper and graphite waveguides.

radius than the above-mentioned 0.1%. This could be important in analyzing the cavity region of gyrotrons that often operate very close to the cutoff frequency of the mode being generated.

The effect of the coupled backward propagating TM_{11} mode on this same mode propagating in the forward direction in a uniform waveguide with a radius near the cutoff radius of the TM_{11} mode can be demonstrated as follows. In the voltage–current formulation of the coupled-mode equations (6) for uniform waveguides ($\theta = 0$), we neglect the effect of coupling, i.e., retain only the $\tau = \nu$ term where ν is the mode designation for the TM_{11} mode. We can then obtain an analytical expression for the propagation constant of the TM_{11} mode, which is identical with that obtained by Jackson [19] for uniform lossy-wall circular waveguides. This expression gives a sensible result even at or below the cutoff radius of the TM_{11} mode. However, if we neglect the effect of the backward coupled mode, the resulting attenuation constant of the TM_{11} mode becomes very large near the cutoff radius.

In varying-radius waveguides with perfectly conducting walls, the coupling coefficients are given by (12) and (13). We see that the coupling coefficients, here, near the cutoff of either mode also become very large. This is because the radial component of the electric field and the axial component of the magnetic field of the TE modes and the azimuthal component of the magnetic field of the TM modes become very large at cutoff. The divergence of the coupling coefficients at cutoff arise due to neglecting the backward propagating modes. In the voltage–current formulation, the coupling coefficients given by (7) are finite everywhere, even at cutoff.

The complex-amplitude coupled-mode equations (10) are not suitable to study the effect of the coupled evanescent modes. In this situation, it is preferable to use the voltage–current formulation of the coupled-mode equations (6), which can incorporate evanescent, as well as propagating modes.

In Fig. 3, the ohmic wall loss per unit length from (27) has been plotted over several beat wavelengths of TE_{11} and TM_{11} modes in a 0.64-cm-diameter copper waveguide. The ohmic wall loss per unit length has been plotted for a graphite waveguide with the same diameter shown in Fig. 4. Graphite has much higher wall resistivity than copper and, hence, can be used in the design of lossy wavguides. As seen from these two figures, at the waveguide input, when the two mode are out-of-

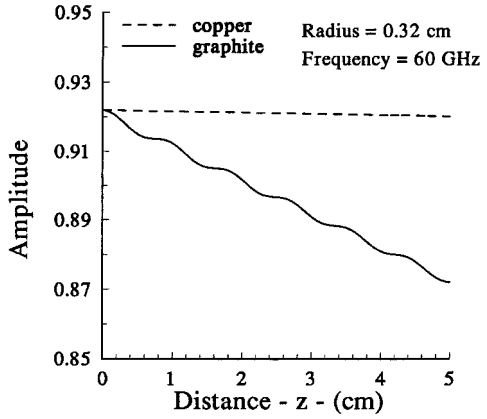

Fig. 8. Amplitude of the TM_{11} mode (of the TE_{11} and TM_{11} combination) along the lossy-wall circular waveguide with 0.64-cm diameter for both copper and graphite waveguides.

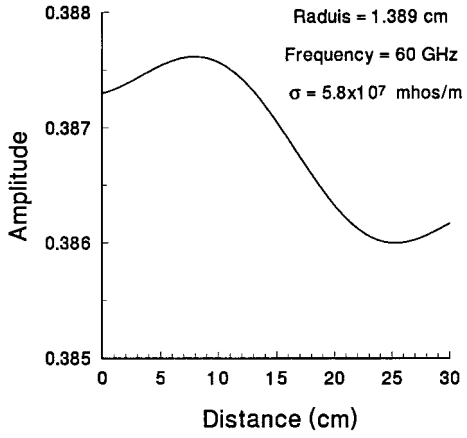

Fig. 9. Amplitude of the TM_{11} mode (of the TE_{11} and TM_{11} combination) along the lossy-wall circular waveguide with 2.779-cm diameter assuming a surface resistivity of ideal copper.

phase, ohmic wall dissipation is very small due to the cancellation of the azimuthal components of the magnetic fields. However, as can be seen from the graph, at approximately half a beat wavelength from the input, the power loss becomes maximum. At this location, the TE_{11} and TM_{11} modes are in-phase and the magnetic-field components add. The pattern then almost repeats itself after each beat wavelength. In these figures, we have also plotted the result obtained by means of the attenuation constants of the two separate modes using the conventional power-loss method which, as seen, incorrectly gives smoothly decaying power loss along the waveguide. In Figs. 5 and 6, the amplitudes of the individual modes are plotted for copper waveguide. Figs. 7 and 8 compare the amplitudes of the individual modes for copper and graphite waveguides. The ripple-like behavior of the curves in Figs. 5–8 arise from the coupling between the modes due to wall loss. If the effect of coupling was neglected, the curves would be smoothly decaying exponential (almost straight lines). In Figs. 9 and 10, we have also plotted the amplitude of the TM_{11} mode in a larger diameter waveguide over a beat wavelength for copper and graphite waveguides, respectively. These curves demonstrate that here the TM_{11} mode actually gains a small amount of power initially from the TE_{11} mode due to ohmic coupling although, as expected, the total power in the two modes monotonically decreases from the initial value.

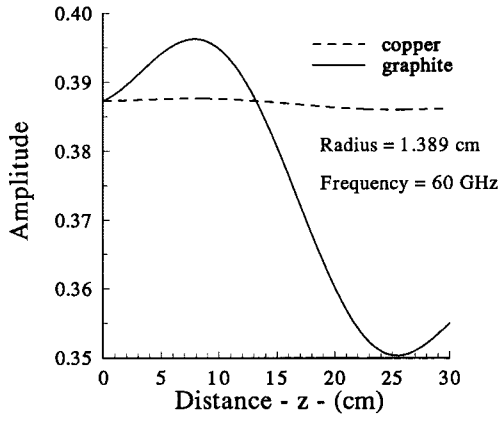

Fig. 10. Amplitude of the TM_{11} mode (of the TE_{11} and TM_{11} combination) along the lossy-wall circular waveguide with 2.779-cm diameter for both copper and graphite waveguides.

VI. Conclusions

In this paper, we have derived the effect of ohmic wall loss on the coupling coefficients in a varying-radius circular waveguide. We have shown that the coupled-mode equations correctly predict that the power loss along the waveguide may vary and, in this case, depends on the relative phases of the modes, as well as their magnitudes. We have shown that, in high-power applications, this effect will lead to the creation of "hot" regions on the waveguide wall for the case of propagation of an HE_{11}-like mode input to a uniform overmoded smooth lossy-wall waveguide. We have shown that the complex-amplitude formulation of the coupled-mode equations for the forward propagating modes is valid for the multimode analysis of uniform waveguides if the waveguide radius is larger than 0.1% above the cutoff radius of the highest order incident mode (in our study, the TM_{11} mode). If the backward coupled modes are also included, the coupled-mode equations are valid even nearer to the cutoff radius.

References

[1] S. E. Miller, "Coupled wave theory and waveguide applications," *Bell Syst. Tech. J.*, pp. 661–719, May 1954.
[2] S. R. Seshadri, "Cylindrical waveguide mode converter for azimuthally symmetric transverse electric modes," *Proc. Inst. Elect. Eng.*, pt. H, vol. 135, no. 6, pp. 420–425, Dec. 1988.
[3] R. A. Schill, Jr. and S. R. Seshadri, "Optimization of a bumpy cylindrical waveguide mode converter," *Int. J. Infrared Millim. Waves*, vol. 7, no. 8, pp. 1129–1167, 1986.
[4] H. G. Unger, "Circular waveguide taper of improved design," *Bell Syst. Tech. J.*, pp. 899–912, July 1958.
[5] J. L. Doane, "Propagation and mode coupling in corrugated and smooth-wall circular waveguide," *Int. J. Infrared Millim. Waves*, vol. 13, pp. 123–170, 1985.
[6] H. Li and M. Thumm, "Mode coupling in corrugated waveguides with varying wall impedance and diameter change," *Int. J. Electron.*, vol. 71, pp. 827–844, 1991.
[7] J. Shafii and R. J. Vernon, "Mode coupling in coaxial waveguides with varying-radius center and outer conductors," *IEEE Trans. Microwave Theory Tech.*, vol. 43, pp. 582–591, Mar. 1995.
[8] T. B. A. Senior, "Impedance boundary conditions for imperfectly conducting surfaces," *Appl. Sci. Res.*, vol. 8, pp. 418–436, 1960.

[9] W. A. Huting and K. J. Webb, "Comparison of mode-matching and differential equation techniques in the analysis of waveguide transitions," *IEEE Trans. Microwave Theory Tech.*, vol. 39, pp. 280–286, Feb. 1991.
[10] W. G. Lawson, "Theoretical evaluation of nonlinear tapers for a high power gyrotrons," *IEEE Trans. Microwave Theory Tech.*, vol. 38, pp. 1617–1622, Nov. 1990.
[11] F. Sporleder and H.-G. Unger, *Waveguide Tapers, Transitions and Couplers*. Stevenage, U.K.: Peregrinus, 1979, sec. 2.6.
[12] G. Strang, *Linear Algebra and its Applications*. New York: Academic, 1976, ch. 5.
[13] J. Shafii and R. J. Vernon, "Mode coupling due to ohmic wall losses in overmoded uniform waveguides—An eigenmode approach," *Int. J. Electron.*, to be published.
[14] J. J. Gustincic, "A general power loss method for attenuation of cavities and waveguides," *IEEE Trans. Microwave Theory Tech.*, vol. MTT-11, pp. 83–87, Jan. 1963.
[15] R. E. Collin, *Foundations for Microwave Engineering*. New York: McGraw-Hill, 1966, ch. 3.
[16] J. L. Doane, "Mode converters for generating the HE_{11} mode from TE_{01} in a circular waveguide," *Int. J. Electron.*, vol. 53, pp. 573–585, 1982.
[17] M. Thumm *et al.*, "Generation of the Gaussian-like HE_{11} mode from gyrotron TE_{0n} mode mixtures at 70 GHz," *Int. J. Infrared Millim. Waves*, vol. 6, pp. 459–470, 1985.
[18] R. E. Collin, *Field Theory of Guided Waves*. New York: McGraw-Hill, 1960, ch. 5.
[19] J. D. Jackson, *Classical Electrodynamic*. New York: Wiley, 1975, sec. 8.6.

Jamal Shafii received the Ph.D. degree in electrical engineering from University of Wisconsin–Madison, in 1994.

His graduate research concerned the development of overmoded waveguide components for high-power microwave transmission. He was recently involved with the development of a mode-converting transmission line for the gyrotron used for electron cyclotron resonance heating (ECRH) on the Helically Symmetric Experiment (HSX) Stellarator at the University of Wisconsin–Madison.

Ronald J. Vernon (S'64–M'65) was born in Chicago, IL. He received the B.S., M.S., and Ph.D. degrees in electrical engineering from Northwestern University, Evanston, IL, in 1959, 1961, and 1965, respectively.

From 1955 to 1958, he worked under a cooperative student program in the Remote Control Engineering Division, Argonne National Laboratory. Since 1965, he has been on the faculty of the University of Wisconsin–Madison, where he is currently a Professor of electrical and computer engineering. He directs a graduate research program in the area of microwaves, antennas, and electromagnetic wave propagation. From 1976 to 1977, he took a sabbatical leave to join the Lawrence Livermore Laboratory, Livermore, CA. His current research interests are in the development of high-power transmission and mode-conversion systems and beam-shaping reflectors for microwave tubes such as gyrotrons.

Dr. Vernon is a member of Sigma Xi, Tau Beta Pi, Eta Kappa Nu, and Pi Mu Epsilon. He was the recipient of the 1998 Gerald Holdridge Award for excellence in teaching.